

Colour Transformations between BVR_c and $g'r'i'$ Photometric Systems for Giant Stars

S. Ak^A, T. Ak^A, S. Karaali^A, S. Bilir^A, S. Tunçel Güçtekin^A, Ö. Önal Taş^A, N. D. Öztürkmen^A, Ş. Duran^A, B. Coşkunoğlu^A, T. Yontan^A, E. Yaz Gökçe^A and Z. Eker^B

^A Istanbul University, Faculty of Sciences, Department of Astronomy and Space Sciences, 34119 University, Istanbul, Turkey, Email: akserap@istanbul.edu.tr

^B Akdeniz University, Faculty of Sciences, Department of Space Sciences and Technologies, 07058, Antalya, Turkey

Abstract: The transformation equations from BVR_c to $g'r'i'$ magnitudes and vice versa for the giants were established from a sample of 80 stars collected from Soubiran et al. (2010) with confirmed surface gravity ($2 \leq \log g$ (cms^{-2}) ≤ 3) at effective temperatures $4000 < T_{\text{eff}}(K) < 16000$. The photometric observations, all sample stars at $g'r'i'$ and 65 of them at BVR_c , were obtained at TÜBİTAK National Observatory (TUG) 1m (T100) telescope, on the Taurus Mountains in Turkey. The M_V absolute magnitudes of the giant stars were estimated from the absolute magnitude-temperature data for the giant stars by Sung et al. (2013) using the T_{eff} from the intrinsic colours considered in this study. The transformation equations could be considered to be valid through the ranges of the following magnitudes and colours involved: $7.10 < V_0 < 14.50$, $7.30 < g'_0 < 14.85$, $-0.20 < (B - V)_0 < 1.41$, $-0.11 < (V - R_c)_0 < 0.73$, $-0.42 < (g' - r')_0 < 1.15$, and $-0.37 < (r' - i')_0 < 0.47$ mag. The transformations were successfully applied to the synthetic BVR_c data of 427 field giants in order to obtain the $g'r'i'$ magnitudes and colours. Comparisons of these data with the $g'r'i'$ observations of giants in this study show that the mean residuals and standard deviations lie within $[-0.010, 0.042]$ and $[0.028, 0.068]$ mag, respectively.

Keywords: techniques: photometric - catalogues - surveys

Introduction

All sky surveys have a great impact on our understanding of the Galactic structure. The optical and longer wavelength surveys give detailed information about the Galactic halo, and Galactic disc and bulge, respectively. The Sloan Digital Sky Survey (SDSS; York et al. 2000) is one of the most widely used sky. Also, it is the largest photometric and spectroscopic survey in the optical wavelengths. Another widely used sky survey is the Two Micron All Sky Survey (2MASS; Skrutskie et al. 2006), which imaged the sky across near-infrared wavelengths. The third sky survey, which is an astrometrically and photometrically important survey, is *Hipparcos* (Perryman et al. 1997), re-reduced by van Leeuwen (2007).

SDSS is based on two sets of passbands, i.e. $u'g'r'i'z'$ and $ugriz$. For the first set, the standard Sloan photometric system was defined on the 1m telescope of the USNO Flagstaff Station (Smith et al. 2002), while a 2.5m telescope was used for the second passband set (Fukugita et al. 1996; Gunn et al. 1998; Hogg et al. 2001). The two sets of passbands are very similar, but not quite identical. However, one can use the transformation equations in the literature to make necessary transformations between two systems (cf. Rider et al. 2004).

It has been customary to derive transformation equations between a newly defined photometric system and the traditional ones, such as the Johnson-Cousins $UBVR_cI_c$ system. Several transformations can be found in the literature related SDSS photometric system (Smith et al. 2002; Karaali, Bilir & Tunçel 2005; Bilir, Karaali & Tunçel 2005; Rodgers et al. 2006; Jordi, Grebel & A 2006; Chonis & Gaskell 2008; Bilir et al. 2008). All these transformations are devoted to dwarfs, the most populated luminosity class in our Galaxy. The two transformations which are carried out for red giants are those of Yaz et al. (2010) and Karaali & Yaz Gökçe (2013).

Yaz et al. (2010) used the JHK_s , BVI , and gri magnitudes in the 2MASS (Cutri et al. 2003), reduced *Hipparcos*' (van Leeuwen 2007) and Ofek's (2008) catalogues and identified two samples of red giants by matching them with the Cayrel de Strobel et al.'s (2001) spectroscopic catalogue which contains the surface gravity $\log g$, a parameter available for dwarf-giant separation. The first sample of stars (91 giants) was used for the transformations between JHK_s and BVI , while the second one (82 giants) was devoted to transformations between JHK_s and gri . The transformations of Karaali & Yaz Gökçe (2013) are based on synthetic

UBV colours of Buser & Kurucz (1992) and synthetic ugr colours of Lenz et al. (1998). They are metallicity and two colours dependent. Three sets of transformation equations are obtained, i.e. for $[M/H] = 0, -1, -2$ dex, which can be interpolated/extrapolated to different metallicities. The advantage of these transformations is that they can be used to extend the colour ranges of the observed $u - g$ and $g - r$ colours which are restricted due to the saturation of the SDSS magnitudes.

In this study, we present transformation equations between either of the most widely used sky surveys, SDSS $g'r'i'$, and BVR_c for giants. The equations are based on the data which were observed and reduced by a team who are included as co-authors in this paper. The sections are organised as follows. Data are presented in Section 2. Section 3 is devoted to the transformation equations and their application and a summary and discussions are given in Section 4.

2 The data

2.1 Observations

The sample consists of fairly bright 80 giants identified and collected by their surface gravities and effective temperatures in the Pastel catalogue (Soubiran et al. 2010): i) $2 \leq \log g$ (cms^{-2}) ≤ 3 , ii) $4000 < T_{\text{eff}}(K) < 16000$. The sample stars cover a large range of metallicities, i.e. $-4 \leq [Fe/H] \leq 0.5$ dex. The sample stars were observed at least three exposures in each filter used. The observations were carried out at 1m RC telescope (T100) at TÜBİTAK National Observatory (TUG)¹ at Bakırli-tepe, Antalya, in Turkey from 2011 July through 2012 September. Table 1 summarizes the journal of observations. The columns indicate the dates, the number of nights, and the number of observing sets at $g'r'i'$ and BVR_c filters both for the sample and standard stars.

Standard reduction techniques were performed with Image Reduction and Analysis Facility (IRAF)². Sky observations during the twilight were used in the flat field corrections. As the dark current level of the CCD camera is very low ($0.0002 \text{ e}^- \text{ pixel}^{-1} \text{ s}^{-1}$) and the exposure times during observing runs are not long, dark current corrections were not applied. Instrumental magnitudes were obtained through aperture photometry using standard IRAF software packages. The instrumental magnitudes and colours were transformed to the standard photometric systems following the procedures described below. The following equations were used for the transformation of the instrumental magnitudes and colours of

giant stars to the standard magnitudes and colours:

$$V = v - k_V \times X_v + \epsilon_V \times (B - V) + \zeta_V \quad (1)$$

$$B - V = \mu \times [(b - v) - (k_{BV} \times X_{BV})] + \zeta_{BV} \quad (2)$$

$$V - R_c = \rho \times [(v - r_c) - (k_{VR_c} \times X_{VR_c})] + \zeta_{VR_c} \quad (3)$$

$$g' = g - k_g \times X_g + \epsilon_g \times (g - r) + \zeta_g \quad (4)$$

$$g' - r' = \kappa \times [(g - r) - (k_{gr} \times X_{gr})] + \zeta_{gr} \quad (5)$$

$$r' - i' = \tau \times [(r - i) - (k_{ri} \times X_{ri})] + \zeta_{ri} \quad (6)$$

where, b, v, r_c and B, V, R_c are the instrumental and the standard magnitudes, respectively. Similarly, g, r, i and g', r', i' denote the instrumental and standard magnitudes for SDSS $u'g'r'i'z'$ photometric system. k and X are photometric extinction coefficient and airmass, respectively, with a subscript denoting the filter or the colour. $\epsilon, \mu, \rho, \kappa$ and τ are the transformation coefficients from the instrumental to the standard, where ζ denotes nightly photometric zeropoint with a subscript indicating the filter or the colour. Using the instrumental magnitudes of the standard stars (Landolt 2009) measured through observations and applying multiple linear least square fits to the equations above, the photometric extinction coefficients, the transformation coefficients and the zeropoint constants were estimated on each night. The averages of them are listed in Table 2. The final standardized photometric data of the sample stars are listed in Table 3. The B, V, R_c observations exist only for 65 sample stars. Therefore, we had to use the synthetic B, V, R_c magnitudes in Pickles & Depagne (2010) to estimate intrinsic $B - V$ and $V - R_c$ colours for the 15 stars which are not observed at BVR_c but observed at $g'r'i'$.

¹www.tug.tubitak.gov.tr

²IRAF is distributed by the National Optical Astronomy Observatories

Table 1: Observing runs at the TUG T100 telescope. Number of frames for giants and standard stars are given in the last four columns according to the filter sets used.

Date	Nights	Giants		Std. stars	
		$g'r'i'$	BVR_c	$g'r'i'$	BVR_c
July 21-23, 2011	3	137	139	187	185
Sept. 9-11, 2011	3	210	187	207	172
Oct. 31-Nov. 01, 2011	2	74	62	91	43
Nov. 21-22, 2011	2	60	45	74	39
Dec. 29, 2011	1	68	—	110	—
Feb. 19, 2012	1	162	—	79	—
Mar. 29, 2012	1	137	—	169	—
Apr. 01, 2012	1	—	57	—	60
Apr. 12, 2012	1	—	56	—	37
Apr. 16-17, 2012	2	88	87	63	56
July 28-29, 2012	2	99	66	203	141
Aug. 18-19, 2012	2	126	121	177	111
Sep. 16-18, 2012	3	248	368	203	203
Total	24	1409	1188	1563	1047

Table 2: Derived average photometric extinction coefficients (k), transformation coefficients (C , see the text), zeropoints (ζ) and average standard deviation (σ) of fits for observing runs. Error values show standard deviation of the measurements.

Magnitude/ colour	k	C	ζ	σ
V	0.137 ± 0.022	-0.076 ± 0.008	-0.753 ± 0.099	0.015 ± 0.007
$B - V$	0.082 ± 0.013	1.191 ± 0.016	-0.012 ± 0.035	0.010 ± 0.003
$V - R_c$	0.044 ± 0.023	0.942 ± 0.009	0.068 ± 0.021	0.008 ± 0.002
g'	0.179 ± 0.048	0.021 ± 0.005	-0.229 ± 0.092	0.016 ± 0.007
$g' - r'$	0.072 ± 0.025	1.035 ± 0.009	-0.247 ± 0.030	0.009 ± 0.003
$r' - i'$	0.058 ± 0.020	0.962 ± 0.023	-0.628 ± 0.029	0.010 ± 0.003

(1) (2)	(3)	(4)	(5)	(6)	(7)	(8)	(9)	(10)	(11)	(12)	(13)	(14)	(15)	(16)	(17)	(18)	(19)	(20)	(21)	(22)	(23)	(24)
ID Star	α (J2000)	δ (J2000)	l	b	$E_d(B - V)$	V	V_{err}	$(B - V)$	$(B - V)_{err}$	$V - R_c$	$(V - R_c)_{err}$	Ref	g'	g'_{err}	$(g' - r')$	$(g' - r')_{err}$	$(r' - i')$	$(r' - i')_{err}$	T_{eff}	$\log g$	$[Fe/H]$	Ref
	(hh:mm:ss.ss)	(dd:mm:ss.ss)	(deg)	(deg)	(mag)	(mag)	(mag)	(mag)	(mag)	(mag)	(mag)		(mag)	(mag)	(mag)	(mag)	(mag)	(mag)	(K)	(cm s^{-2})	(dex)	
61 NGC 6341 12018	17 17 22.38	+43 06 56.34	68.320	34.811	0.019	14.432	0.008	0.672	0.013	0.428	0.011	1	14.849	0.009	0.564	0.011	0.220	0.008	5160	2.30	-2.34	2000AJ...120.1351S
62 HD 170737	18 29 54.11	+26 39 26.24	55.019	16.213	0.043	8.117	0.011	0.804	0.011	0.462	0.011	1	8.472	0.001	0.597	0.001	0.240	0.001	5100	3.30	-0.68	2012A&A...541A.157S
63 BD+05 3839	18 37 34.21	+05 28 33.46	36.243	5.572	0.229	9.397	0.002	1.190	0.003	0.606	0.003	1	9.904	0.002	0.906	0.003	0.371	0.003	5100	2.83	-0.01	1994ApJS...91..309L
64 BD+05 3858	18 38 20.75	+05 26 02.31	36.293	5.380	0.207	9.358	0.002	1.066	0.003	0.534	0.003	1	9.804	0.002	0.788	0.003	0.329	0.003	5200	3.00	-0.03	1994ApJS...91..309L
65 HD 175305	18 47 06.44	+74 43 31.45	105.834	26.379	0.048	7.252	0.001	0.772	0.001	0.473	0.002	1	7.543	0.001	0.569	0.001	0.196	0.001	5036	2.76	-1.35	2012ApJ...753...64I
66 NGC 6705 1423	18 50 55.82	-06 18 14.80	27.259	-2.758	0.318	11.454	0.003	1.634	0.006	0.853	0.004	1	12.178	0.003	1.316	0.004	0.513	0.002	4750	2.90	0.04	2006AJ...131.2949S
67 NGC 6705 1256	18 51 00.24	-06 16 59.50	27.286	-2.764	0.372	11.626	0.004	1.699	0.009	0.909	0.004	1	12.387	0.004	1.403	0.004	0.572	0.003	4600	2.50	0.28	2006AJ...131.2949S
68 NGC 6705 1223	18 51 00.93	-06 14 56.40	27.318	-2.751	0.356	11.480	0.003	1.230	0.005	0.693	0.004	1	12.030	0.003	1.006	0.004	0.423	0.003	4750	2.50	-0.06	2006AJ...131.2949S
69 BD+05 4314	19 51 49.60	+05 36 45.84	44.989	-10.725	0.119	10.757	0.002	0.779	0.003	0.459	0.003	1	11.079	0.002	0.575	0.003	0.218	0.003	5000	3.00	-1.51	2003PASP...115...22Y
70 NGC 6838 1056	19 53 48.40	+18 48 23.50	56.773	-4.557	0.257	13.251	0.005	1.339	0.010	0.741	0.006	1	13.931	0.004	1.124	0.004	0.485	0.003	4582	2.10	-0.77	1986A&A...169..208G
71 BD-14 5890	20 56 09.13	-13 31 17.66	34.408	-33.683	0.030	10.192	0.002	0.803	0.003	0.478	0.002	1	10.517	0.001	0.653	0.002	0.230	0.003	4891	2.03	-2.16	2012ApJ...753...64I
72 BD-03 5215	21 28 01.31	-03 07 40.93	50.075	-35.866	0.048	10.123	0.005	0.613	0.005	0.368	0.006	1	10.384	0.004	0.427	0.005	0.176	0.005	5478	2.17	-1.49	2012ApJ...753...64I
73 BPS CS 22944-032	21 47 43.10	-13 40 22.00	40.906	-45.175	0.038	13.161	0.003	0.597	0.004	0.390	0.004	1	13.433	0.002	0.482	0.003	0.196	0.003	5300	2.87	-2.98	2008ApJ...681.1524L
74 HD 210295	22 09 41.44	-13 36 19.47	44.406	-49.964	0.035	9.455	0.002	0.847	0.002	0.469	0.002	1	9.937	0.001	0.719	0.001	0.254	0.002	4763	2.19	-1.25	2012ApJ...753...64I
75 HD 219715	23 18 01.19	+09 04 28.11	87.675	-47.301	0.050	9.197	0.002	0.779	0.003	0.456	0.003	1	9.733	0.004	0.566	0.005	0.213	0.004	5000	2.50	-1.10	2000A&A...353..978M
76 NGC 7789 329	23 56 55.46	+56 45 09.10	115.477	-5.328	0.313	12.307	0.003	1.433	0.007	0.774	0.004	1	12.999	0.005	1.208	0.005	0.489	0.003	4345	2.20	0.10	1985PASP...97..801P
77 NGC 7789 353	23 56 57.52	+56 45 27.30	115.483	-5.324	0.326	12.612	0.004	1.432	0.009	0.784	0.004	1	13.303	0.006	1.206	0.007	0.487	0.004	4345	2.20	0.15	1985PASP...97..801P
78 NGC 7789 637	23 57 22.43	+56 41 46.00	115.526	-5.396	0.313	12.419	0.003	1.457	0.008	0.784	0.004	1	13.118	0.006	1.222	0.007	0.513	0.004	4383	2.10	0.00	1985PASP...97..801P
79 NGC 7789 737	23 57 29.97	+56 43 19.90	115.548	-5.374	0.327	13.383	0.007	1.179	0.016	0.645	0.008	1	13.996	0.013	0.999	0.014	0.396	0.008	4990	2.80	-0.10	1985PASP...97..801P
80 NGC 7789 765	23 57 31.87	+56 41 22.12	115.546	-5.407	0.275	11.634	0.002	1.499	0.004	0.800	0.002	1	12.325	0.003	1.223	0.003	0.515	0.001	4383	2.10	-0.20	1985PASP...97..801P

(1) This study, (2) Pickles & Depagne (2010)

2.2 Distances and De-reddening of the Magnitudes and Colours

After obtaining standardized observed magnitudes and colours of the present sample of giants (80) through Eqs. 1 to 6, de-reddening of them is the next step before attempting to establish the transformation equations between BVR_c and $g'r'i'$. A primary advantage for us to know calibrated absolute magnitudes of giants from the tables of Sung et al. (2013). Sung et al. (2013) have studied spectral type- M_V and spectral type- T_{eff} relation of giants in general along with other luminosity classes on the H-R diagram in the Johnson-Cousins $UBVR_cI_c$ system. Using their Table 4 and 5, we have plotted absolute magnitudes as a function of the effective temperature. The data existing on these tables in the range of $3600 < T_{eff}(K) \leq 16000$ were shown by filled circles in Fig. 1. In order to increase efficient use of the data, two polynomial functions were fitted to the cooler ($3600 < T_{eff}(K) \leq 6000$) and to the hotter ($6000 < T_{eff}(K) < 16000$) regions. Dashed line in Fig. 1 represents the polynomials fitted.

For a given effective temperature of our sample giants as supplied by the Pastel catalogue (Soubiran et al. 2010), the absolute magnitude (M_V) is provided by Fig. 1. Nevertheless, absolute magnitude alone is not enough to estimate neither the distance nor the interstellar extinction. The total interstellar absorption in V -band could be estimated by means of the maps of Schlafly & Finkbeiner (2011) which are based on a recalibration of the Schlegel, Finkbeiner & Davis (1998) maps, for each of the sample star, by including the Galactic coordinates of the star in question into the NED service³. The value A_∞ is valid for a star at infinite distance. However, we used it in the Pogson's equation and evaluated the distance to the star as a first approximation:

$$V - M_V - A_\infty = 5 \log d - 5, \quad (7)$$

where V and M_V are the apparent and the absolute magnitudes from which the distance is estimated. We then reduced A_∞ to the total absorption of the star at distance d , i.e. A_d , by the procedure of Bahcall & Soneira (1980). We have replaced the numerical value of $A_d(b)$ with the one of A_∞ in Eq. (7), and applied a series of iteration to obtain the final total absorption A_V by which the selective absorption (colour excess), $E_d(B - V)$ could be evaluated for distance d as follows:

$$E_d(B - V) = A_d(b) / 3.1. \quad (8)$$

$E_d(B - V)$ is the standard $E(B - V)$ colour excess of the star with given V , M_V and d , from which one can compute

³<http://ned.ipac.caltech.edu/forms/calculator.html>

Table 5: Mean values of the errors for magnitude and colours in the BVR_c and $g'r'i'$ systems.

Magnitude/ Colour	Mean Error (mag)	Magnitude/ Colour	Mean Error (mag)
V	0.003	g'	0.003
$B - V$	0.005	$g' - r'$	0.003
$V - R_c$	0.004	$r' - i'$	0.003

intrinsic colour by using observed colour and de-reddened observed magnitude. The range of the colour excess of the sample stars is $0 < E(B - V) < 0.84$ mag, and their distribution in the Galactic longitude-Galactic latitude plane is plotted in Fig. 2, where one may notice the $E(B - V)$ colour excess is highest on the Galactic plane and decreases towards the Galactic poles. We have made consistency check of $E(B - V)$ colour excesses of 25 giant stars by comparing the colour excesses of the clusters which they belong to. The results are given in Table 4, where the columns are explanatory to indicate the name of the cluster, the star's ID, equatorial coordinates (J2000), the colour excesses $E_d(B - V)$ of the stars estimated in this study and the colour excess $E_{cl}(B - V)$ of the cluster from the literature. The colour excesses $E_{cl}(B - V)$ of the clusters NGC 6341 and NGC 6838 are taken from Harris (1996, edition 2010), while those for the remaining five clusters are provided from Dias et al. (2002). Table 4 shows that the colour excesses evaluated in this study and taken from literature are in good agreement, in general.

The magnitudes and colours are de-reddened by using the corresponding $E(B - V)$ colour excess of the star and the equations in the literature, i.e. we adopted $A_V/E(B - V)=3.1$, $E(V - R_c)/E(B - V)=0.65$ (Cardelli, Clayton & Mathis 1989) and $A_{g'}/A_V=1.199$, $A_{r'}/A_V=0.858$, $A_{i'}/A_V=0.639$ (Fan 1999). The two colour-diagrams for the sample stars are plotted with symbols in Fig. 3 and Fig. 4 for Johnson-Cousins and SDSS systems, respectively. The solid curves in Fig. 3 and Fig. 4 are adopted from the synthetic data in Pickles (1998) and in Covey et al. (2007), respectively. The mean errors of the observed magnitude and colours of both systems are given in Table 5 and plotted in Fig. 5.

3 Transformations

The following general equations have been preferred to derive the 18 sets of transformation equations with their coefficients between BVR_c and $g'r'i'$ photometric systems using de-reddened magnitudes and colours of the sample giants in this study. Eqs. (9)-(17) transform BVR_c into $g'r'i'$ magnitudes and colours, while Eqs. (18)-(26) are their inverse

Table 4: The colour excesses of the stars observed in various stellar clusters. Cluster names, star IDs, equatorial coordinates and evaluated colour excesses ($E_d(B - V)$) of stars are given in columns 1-5. The last two columns include colour excesses ($E_{cl}(B - V)$) of the clusters and their reference.

Cluster	Star	α (J2000) (hh:mm:ss.ss)	δ (J2000) (dd:mm:ss.ss)	$E_d(B - V)$ (mag)	$E_{cl}(B - V)$ (mag)	Reference
NGC 2112	204	05 53 47.54	+00 22 02.00	0.793	0.600	Dias et al. (2002)
	402	05 53 53.30	+00 24 37.90	0.839	0.600	Dias et al. (2002)
NGC 2420	115	07 38 21.67	+21 33 51.40	0.036	0.040	Dias et al. (2002)
	173	07 38 26.96	+21 33 31.30	0.036	0.040	Dias et al. (2002)
NGC 2682	84	08 51 12.70	+11 52 42.40	0.030	0.040	Dias et al. (2002)
	105	08 51 17.10	+11 48 16.10	0.030	0.040	Dias et al. (2002)
	141	08 51 22.80	+11 48 01.70	0.030	0.040	Dias et al. (2002)
	151	08 51 26.19	+11 53 52.00	0.031	0.040	Dias et al. (2002)
	164	08 51 28.99	+11 50 33.10	0.031	0.040	Dias et al. (2002)
	224	08 51 43.55	+11 44 26.40	0.025	0.040	Dias et al. (2002)
	231	08 51 45.08	+11 47 45.90	0.027	0.040	Dias et al. (2002)
	266	08 51 59.52	+11 55 04.90	0.032	0.040	Dias et al. (2002)
NGC 6341	9012	17 16 52.84	+43 03 29.50	0.020	0.020	Harris (1996)
	10065	17 17 11.41	+43 06 02.70	0.019	0.020	Harris (1996)
	11027	17 17 21.61	+43 06 15.90	0.019	0.020	Harris (1996)
	12018	17 17 22.38	+43 06 56.34	0.019	0.020	Harris (1996)
NGC 6705	1423	18 50 55.82	-06 18 14.80	0.318	0.428	Dias et al. (2002)
	1256	18 51 00.24	-06 16 59.50	0.372	0.428	Dias et al. (2002)
	1223	18 51 00.93	-06 14 56.40	0.356	0.428	Dias et al. (2002)
NGC 6838	1056	19 53 48.40	+18 48 23.50	0.257	0.250	Harris (1996)
NGC 7789	329	23 56 55.46	+56 45 09.10	0.313	0.280	Dias et al. (2002)
	353	23 56 57.52	+56 45 27.30	0.326	0.280	Dias et al. (2002)
	637	23 57 22.43	+56 41 46.00	0.313	0.280	Dias et al. (2002)
	737	23 57 29.97	+56 43 19.90	0.327	0.280	Dias et al. (2002)
	765	23 57 31.87	+56 41 22.12	0.275	0.280	Dias et al. (2002)

transformations. The equations are:

$$(g' - V)_0 = a_i(B - V)_0^2 + b_i(B - V)_0 + c_i \quad (9)$$

$$(g' - V)_0 = a_i(V - R_c)_0^2 + b_i(V - R_c)_0 + c_i \quad (10)$$

$$(g' - V)_0 = a_i(B - V)_0 + b_i(V - R_c)_0 + c_i \quad (11)$$

$$(g' - r')_0 = a_i(B - V)_0^2 + b_i(B - V)_0 + c_i \quad (12)$$

$$(g' - r')_0 = a_i(V - R_c)_0^2 + b_i(V - R_c)_0 + c_i \quad (13)$$

$$(g' - r')_0 = a_i(B - V)_0 + b_i(V - R_c)_0 + c_i \quad (14)$$

$$(r' - i')_0 = a_i(B - V)_0^2 + b_i(B - V)_0 + c_i \quad (15)$$

$$(r' - i')_0 = a_i(V - R_c)_0^2 + b_i(V - R_c)_0 + c_i \quad (16)$$

$$(r' - i')_0 = a_i(B - V)_0 + b_i(V - R_c)_0 + c_i \quad (17)$$

$$(V - g')_0 = d_i(g' - r')_0^2 + e_i(g' - r')_0 + f_i \quad (18)$$

$$(V - g')_0 = d_i(r' - i')_0^2 + e_i(r' - i')_0 + f_i \quad (19)$$

$$(V - g')_0 = d_i(g' - r')_0 + e_i(r' - i')_0 + f_i \quad (20)$$

$$(B - V)_0 = d_i(g' - r')_0^2 + e_i(g' - r')_0 + f_i \quad (21)$$

$$(B - V)_0 = d_i(r' - i')_0^2 + e_i(r' - i')_0 + f_i \quad (22)$$

$$(B - V)_0 = d_i(g' - r')_0 + e_i(r' - i')_0 + f_i \quad (23)$$

$$(V - R_c)_0 = d_i(g' - r')_0^2 + e_i(g' - r')_0 + f_i \quad (24)$$

$$(V - R_c)_0 = d_i(r' - i')_0^2 + e_i(r' - i')_0 + f_i \quad (25)$$

$$(V - R_c)_0 = d_i(g' - r')_0 + e_i(r' - i')_0 + f_i \quad (26)$$

The values of the coefficients and their errors are given in Table 6 and Table 7. The distribution of the sample stars on the colour planes are plotted in Fig. 6. The ranges of the magnitudes and colours in the transformations are: $7.10 < V_0 < 14.50$, $7.30 < g_0 < 14.85$, $-0.20 < (B - V)_0 < 1.41$, $-0.11 < (V - R_c)_0 < 0.73$, $-0.42 < (g - r)_0 < 1.15$, and $-0.37 < (r - i)_0 < 0.47$ mag. The residuals of the colours from the curve fits are plotted in Fig. 7 and Fig. 8, while the means and standard deviations of the residuals are included to the data in Tables 6 and 7.

The transformation equations from BVR_c to $g'r'i'$ colours derived in this study have been applied to another sample of 427 giants taken from Pickles & Depagne (2010) as explained in the following. Smith et al. (2005) have published a list of ~ 16000 southern SDSS standards, which includes some repetition. 6117 of them were turned out to be of luminosity class III, i.e. giants, which cover the spectral range A-M. We have selected a sample of 427 giants with uncertainties in g' , r' and i' less than 0.01 mag. The $E(B - V)$ colour excesses used for de-reddening the g' magnitudes, and $g' - r'$ and $r' - i'$ colours have been evaluated in two steps, by a procedure similar to the

one used for the original sample from which the Eqs. 7 and 8 derived as in Section 2.2. The g' magnitudes, and $g' - r'$ and $r' - i'$ colours are de-reddened according to the corresponding $E(B - V)$ colour excesses of the stars and the equations of Fan (1999). The $(g' - r')_0 \times (r' - i')_0$ two-colour diagram of the sample of 427 stars obtained from Pickles & Depagne (2010) are given in Fig. 9.

To estimate intrinsic BVR_c colours of the sample of those 427 giants, we have identified them first in Pickles & Depagne (2010), and then recorded their V magnitudes and, $B - V$ and $V - R_c$ colours. Then, those V magnitudes and, $B - V$ and $V - R_c$ colours are de-reddened by the procedure explained in the Section 2.2, and transformed them to g'_0 magnitudes and, $(g' - r')_0$ and $(r' - i')_0$ colours by using the transformation equations derived from the original sample of 80 giants in this study. Then, we have compared those g'_0 magnitude and, $(g' - r')_0$ and $(r' - i')_0$ colours obtained through transformation equations to the g'_0 magnitude and, $(g' - r')_0$ and $(r' - i')_0$ colours evaluated from Pickles & Depagne (2010). The residuals, i.e. the differences between the original and evaluated colours, are plotted in Fig. 10. The mean and standard deviations of the residuals for each colour are also indicated in the corresponding panel of the figure.

4 Summary and Discussion

The transformation equations from BVR_c to $g'r'i'$ colours and vice versa for giants were derived and presented. The transformation equations were obtained using the observed magnitudes and colours of a sample of 80 giants selected from the Pastel catalogue (Soubiran et al. 2010) with confirmed surface gravity ($2 \leq \log g \text{ (cms}^{-2}\text{)} \leq 3$) at effective temperatures from 4000 to 16000 K. The $g'r'i'$ magnitudes of all sample and 65 of them at BVR_c magnitudes were obtained by observations carried out with the T100 telescope at TUG at Bakrlhtepe, Antalya, in the years 2011-2012. The BVR_c magnitudes of 15 giants were completed from the synthetic BVR_c magnitudes in Pickles & Depagne (2010). We have used the M_V absolute magnitudes and T_{eff} temperatures for giants at various spectral types presented in Sung et al. (2013) to produce Fig. 1, which were used to estimated the M_V absolute magnitudes of the sample stars used in this study. We have de-reddened the magnitude and colours in both photometric systems, BVR_c and $g'r'i'$ of the sample by a procedure commonly used in the literature.

The transformation equations from BVR_c to $g'r'i'$ (Eqs. 9-17) and inverse transformations (Eqs. 18-26) were derived by fitting quadratic polynomials to $(g' - V)_0$, $(g' - r')_0$ and $(r' - i')_0$ which are given in terms of $(B - V)_0$ only or $(V - R_c)_0$ only, or by fitting a linear function to them if they are ex-

Table 6: Coefficients for the Eqs. (9)-(17). The figures in the first line indicate the equation number, R is the correlation coefficient and, s and $m.r.$ are the standard deviation, and mean residuals, respectively.

	(9)	(10)	(11)	(12)	(13)
Coefficient	$(g' - V)_0$	$(g' - V)_0$	$(g' - V)_0$	$(g' - r')_0$	$(g' - r')_0$
a_i	-0.122 ± 0.051	-0.155 ± 0.227	0.404 ± 0.083	-0.045 ± 0.031	0.381 ± 0.120
b_i	0.651 ± 0.074	1.044 ± 0.160	0.168 ± 0.166	1.006 ± 0.055	1.528 ± 0.055
c_i	-0.069 ± 0.028	-0.056 ± 0.032	-0.035 ± 0.024	-0.197 ± 0.024	-0.170 ± 0.009
R	0.912	0.876	0.907	0.986	0.992
s	0.068	0.080	0.070	0.059	0.059
$m.r.$	0.000	0.000	0.000	-0.006	-0.002
	(14)	(15)	(16)	(17)	
Coefficient	$(g' - r')_0$	$(r' - i')_0$	$(r' - i')_0$	$(r' - i')_0$	
a_i	0.464 ± 0.063	-0.243 ± 0.035	-0.420 ± 0.064	-0.026 ± 0.049	
b_i	0.931 ± 0.128	0.730 ± 0.051	1.111 ± 0.030	0.897 ± 0.099	
c_i	-0.205 ± 0.018	-0.224 ± 0.019	-0.209 ± 0.005	-0.185 ± 0.014	
R	0.982	0.940	0.993	0.953	
s	0.054	0.047	0.031	0.042	
$m.r.$	0.000	0.000	-0.001	0.000	

Table 7: Coefficients for the Eqs. (18)-(26). The symbols are as in Table 6.

	(18)	(19)	(20)	(21)	(22)
Coefficient	$(V - g')_0$	$(V - g')_0$	$(V - g')_0$	$(B - V)_0$	$(B - V)_0$
d_i	0.041 ± 0.016	-0.104 ± 0.165	-0.460 ± 0.059	0.022 ± 0.018	0.466 ± 0.117
e_i	-0.615 ± 0.013	-1.096 ± 0.029	-0.243 ± 0.111	1.028 ± 0.014	1.947 ± 0.028
f_i	-0.030 ± 0.007	-0.156 ± 0.014	-0.052 ± 0.015	0.205 ± 0.007	0.418 ± 0.015
R	0.989	0.977	0.989	0.996	0.987
s	0.049	0.067	0.050	0.055	0.098
$m.r.$	0.001	-0.001	-0.005	0.002	0.005
	(23)	(24)	(25)	(26)	
Coefficient	$(B - V)_0$	$(V - R_c)_0$	$(V - R_c)_0$	$(V - R_c)_0$	
d_i	1.321 ± 0.092	-0.002 ± 0.016	0.102 ± 0.097	0.335 ± 0.037	
e_i	-0.616 ± 0.193	0.552 ± 0.009	1.085 ± 0.017	0.449 ± 0.068	
f_i	0.162 ± 0.023	0.112 ± 0.004	0.229 ± 0.009	0.158 ± 0.009	
R	0.974	0.992	0.991	0.995	
s	0.071	0.033	0.039	0.030	
$m.r.$	0.000	0.007	0.001	0.002	

pressed both $(B - V)_0$ and $(V - R_c)_0$. Similarly, $(V - g')_0$, $(B - V)_0$ and $(V - R_c)_0$ expressed by a quadratic function of $(g' - r')_0$ or $(r' - i')_0$, or they are expressed by a linear function fit both $(g' - r')_0$ and $(r' - i')_0$ colours used in the equation. The correlation coefficients and the standard deviations in Table 6 show that all the transformation equations (Eqs. 9-17) provide sufficiently accurate magnitude and colours. However, the most accurate colours $(g' - V)_0$, $(g' - r')_0$ and $(r' - i')_0$ come from the quadratic equations containing only $(B - V)_0$, or $(V - R_c)_0$. The correlation coefficients given in Table 7 for inverse transformations are a bit larger, while the standard deviations are smaller. The most accurate colours $(V - g')_0$, $(B - V)_0$, and $(V - R)_0$ come from the quadratic equations containing only $(g' - r')_0$, or $(g' - r')_0$ and from the linear equation if both $(g' - r')_0$ and $(g' - r')_0$ appear in the equation.

The transformation equations could be considered valid for the ranges of the magnitudes and colours used in the transformations: $7.10 < V_0 < 14.50$, $7.30 < g'_0 < 14.85$, $-0.20 < (B - V)_0 < 1.41$, $-0.11 < (V - R_c)_0 < 0.73$, $-0.42 < (g' - r')_0 < 1.15$, and $-0.37 < (r' - i')_0 < 0.47$ mag, rather larger than the ones provided by Yaz et al. (2010), i.e. $0.25 < (B - V)_0 < 1.35$, $0.10 < (g - r)_0 < 0.95$, and $0 < (r - i)_0 < 0.35$.

We applied the transformation equations derived in this study to the synthetic BVR_c data of 427 giants taken from Pickles & Depagne (2010). The ranges of the mean residuals ($m.r.$) and standard deviations (s) are $-0.010 \leq m.r. \leq 0.042$ and $0.028 \leq s \leq 0.068$ mag, respectively. That is, the g' magnitude and, $(g' - r')_0$ and $(r' - i')_0$ colours of a giant can be estimated by our transformations with an accuracy of at least ~ 0.05 mag. Yaz et al. (2010) derived transformations between 2MASS, SDSS and BVI photometric systems for late type giants for two cases, i.e. metallicity dependent and free of metallicity. We have compared their residuals and the standard deviations free of metallicity. Their mean residuals are rather small, i.e. $-0.0005 \leq m.r. \leq 0.0004$ mag. However, the corresponding standard deviations are larger than the ones in our study, $0.075 \leq s \leq 0.167$ mag. That is, our study provides magnitudes and colours with an accuracy of ~ 1.5 times that of Yaz et al. (2010).

Sufficiently small residuals and the standard deviations confirm the quality of the observations made in TUG, and accuracy and the precision of the reductions applied to these observations. The metallicities of the sample stars used for deriving the coefficients of the transformation equations between the two photometric systems cover a large range, $-4 \leq [Fe/H] \leq 0.5$ dex. However, the number of stars with $[Fe/H] < -1$ dex are small. Hence, we did not consider the metallicity in our transformations. Though, we obtained transformation

equations which provide accurate colour and magnitudes.

5 Acknowledgments

This work has been supported in part by the Scientific and Technological Research Council (TÜBİTAK) 212T214.

We thank to TÜBİTAK for a partial support in using T100 telescope with project number 11BT100-184-2.

This research has made use of the NASA/IPAC Infrared Science Archive and Extragalactic Database (NED) which are operated by the Jet Propulsion Laboratory, California Institute of Technology, under contract with the National Aeronautics and Space Administration.

This research has made use of the SIMBAD, and NASA's Astrophysics Data System Bibliographic Services.

References

- Bahcall J.N., Soneira R.M., 1980, ApJS, 44, 73
- Bilir S., Karaali S., Tunçel S., 2005, AN, 326, 321
- Bilir S., Ak S., Karaali S., Cabrera-Lavers A., Chonis T.S., Gaskell C.M., 2008, MNRAS, 384, 1178
- Buser R., Kurucz R.L., 1992, A&A, 264, 557
- Cardelli J.A., Clayton G.C., Mathis J.S., 1989, ApJ, 345, 245
- Cayrel de Strobel G., Soubiran C., Ralite N., 2001, A&A, 373, 159
- Chonis T.S., Gaskell C.M., 2008, AJ, 135, 264
- Covey K.R., et al., 2007, AJ, 134, 2398
- Cutri R.M., et al., 2003, 2MASS All-Sky Catalog of Point Sources, CDS/ADC Electronic Catalogues 2246
- Dias W.S., Alessi B.S., Moitinho, A., Lepine, J.R.D., 2002, A&A, 389, 871
- Fan X., 1999, AJ, 117, 2528
- Fukugita M., Ichikawa T., Gunn J.E., Doi M., Shimasaku K., Schneider D. P., 1996, AJ, 111, 1748
- Gunn J.E., et al., 1998, AJ, 116, 3040
- Harris W.E., 1996. AJ, 112, 1487
- Hogg D.W., Finkbeiner D.P., Schlegel D.J., Gunn J.E., 2001, AJ, 122, 2129
- Jordi K., Grebel E. K., Ammon K., 2006, A&A, 460, 339

- Karaali S., Bilir S., Tunçel S., 2005, PASA, 22, 24
- Karaali S., Yaz Gökçe E., 2013, PASA, 20, 30
- Landolt A.U., 2009, AJ, 137, 4186
- Lenz D.D., Newberg J., Rosner R., Richards G.T., Stoughton C., 1998, ApJS, 119, 121
- Ofek E.O., 2008, PASP, 120, 1128
- Perryman M.A.C., et al., 1997, A&A, 323L, 49
- Pickles A.J., 1998, PASP, 110, 863
- Pickles A., Depagne É., 2010, PASP, 122, 1437
- Rider C.J., Tucker D.L., Smith J.A., Stoughton C., Allam S.S., Neilsen E.H., 2004, AJ, 127, 2210
- Rodgers C.T., Canterna R., Smith J.A., Pierce M.J., Tucker D.L., 2006, AJ, 132, 989
- Schlafly E.F., Finkbeiner D.P., 2011, ApJ, 737, 103
- Schlegel D. J., Finkbeiner D. P., Davis M., 1998, ApJ, 500, 525
- Skrutskie M.F., et al., 2006, AJ, 131, 1163
- Smith J.A., et al., 2002, AJ, 123, 2121
- Smith J.A., et al., 2005, AAS, 20713111
- Soubiran C., Le Campion J.-F., Cayrel de Strobel G., Caillo A., 2010, A&A, 515, A111
- Sung H., Lim B., Bessell M.S., Kim J. S., Hur H., Chun M., Park B., 2013, JKAS, 46, 103
- van Leeuwen, F., 2007, A&A, 474, 653
- Yaz E., Bilir S., Karaali S., Ak S., Coşkunoglu B., Cabrera-Lavers A., 2010, AN, 331, 807
- York D.G., et al., 2000, AJ, 120, 1579

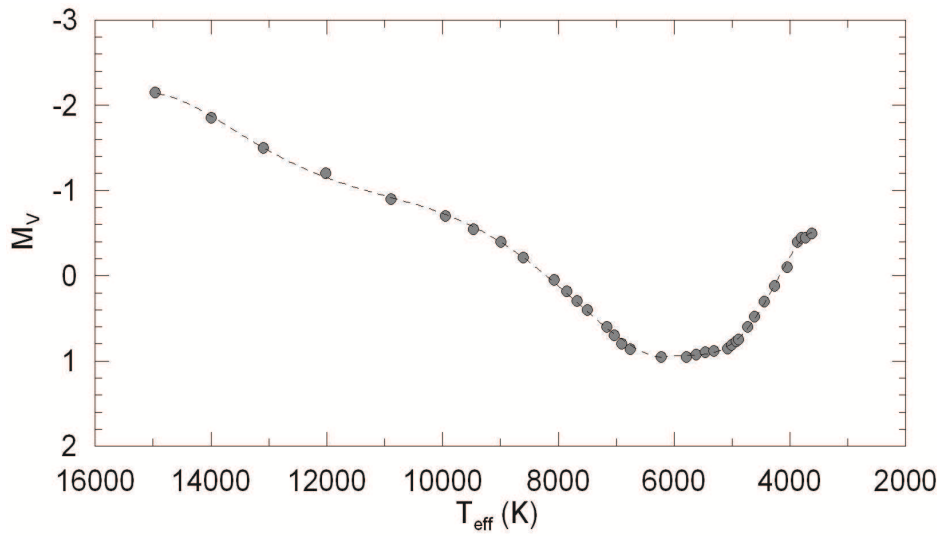


Figure 1: $M_V \times T_{\text{eff}}$ absolute magnitude-temperature diagram for the giant stars in Sung et al. (2013) which is used for absolute magnitude estimation of the sample stars.

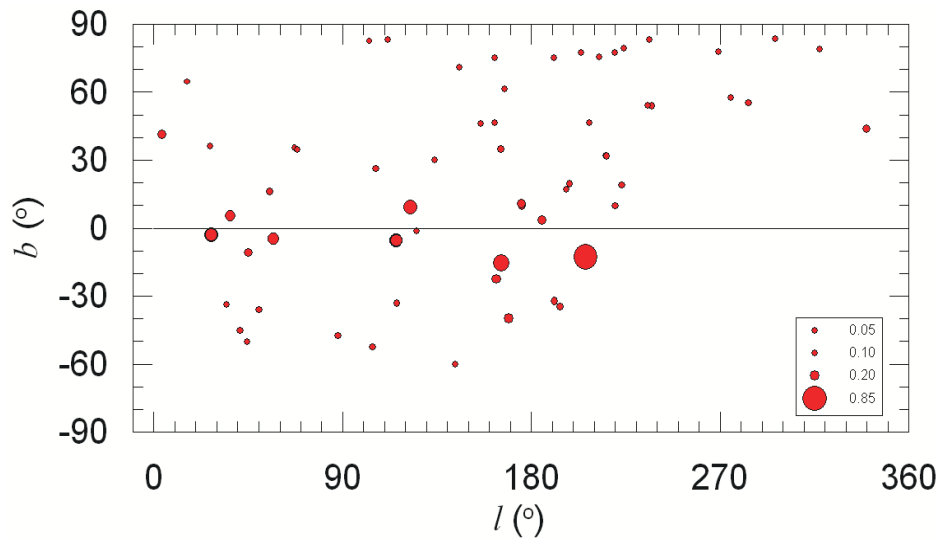


Figure 2: Galactic coordinates of the programme stars observed in TUG. The radius of the circles are proportional to the $E(B - V)$ colour excess of the star.

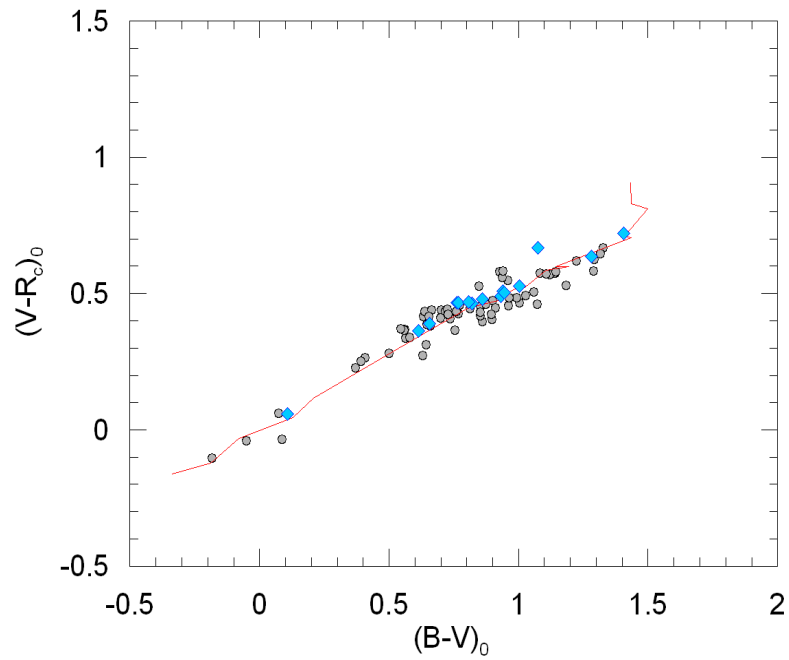


Figure 3: $(B-V)_0 \times (V-R_c)_0$ two-colour diagram of the sample stars. The positions of 15 stars with synthetic $(B-V)_0$ and $(V-R_c)_0$ colours are marked with a different symbol (\diamond). The solid line indicates the synthetic two-colour diagram of Pickles (1998).

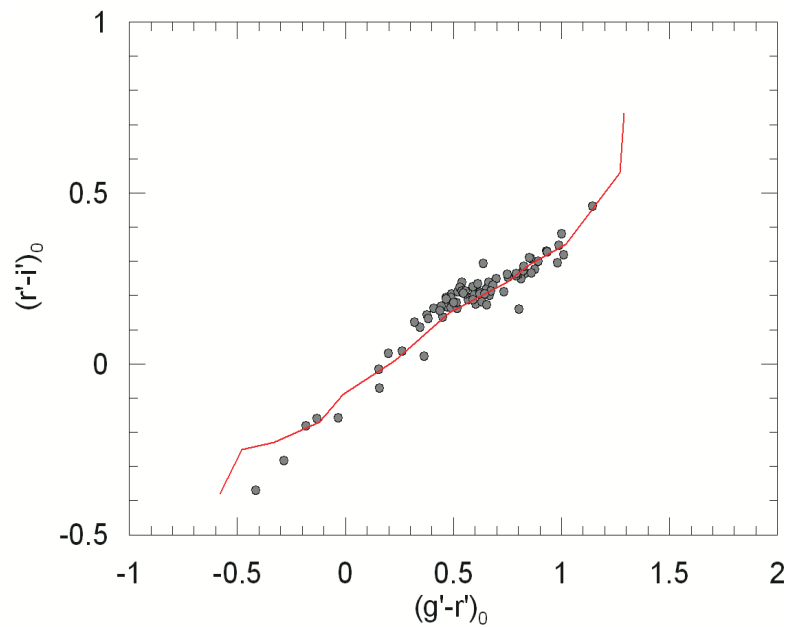


Figure 4: $(g'-r')_0 \times (r'-i')_0$ two-colour diagram of the sample stars. The solid line indicates the synthetic two-colour diagram of Covey et al. (2007).

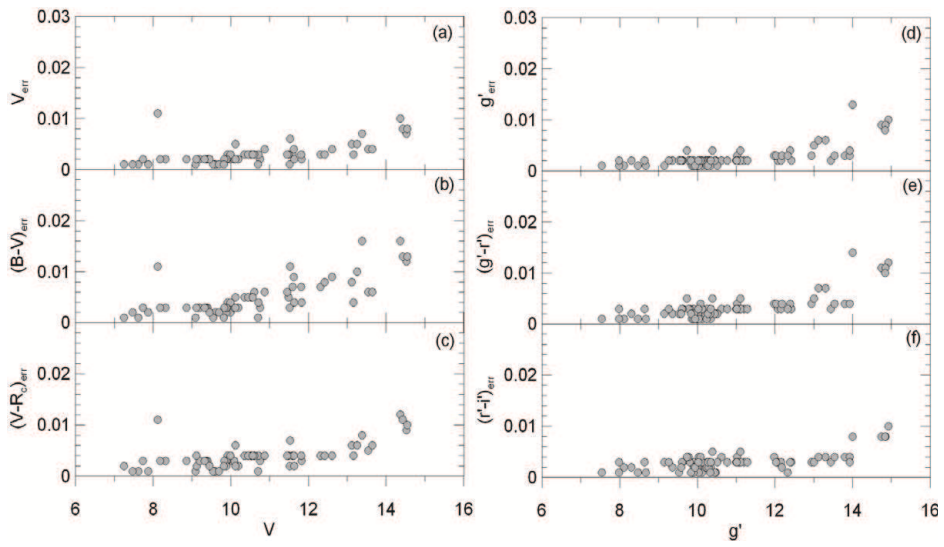


Figure 5: Distributions of the errors of the magnitudes and colours of the sample stars.

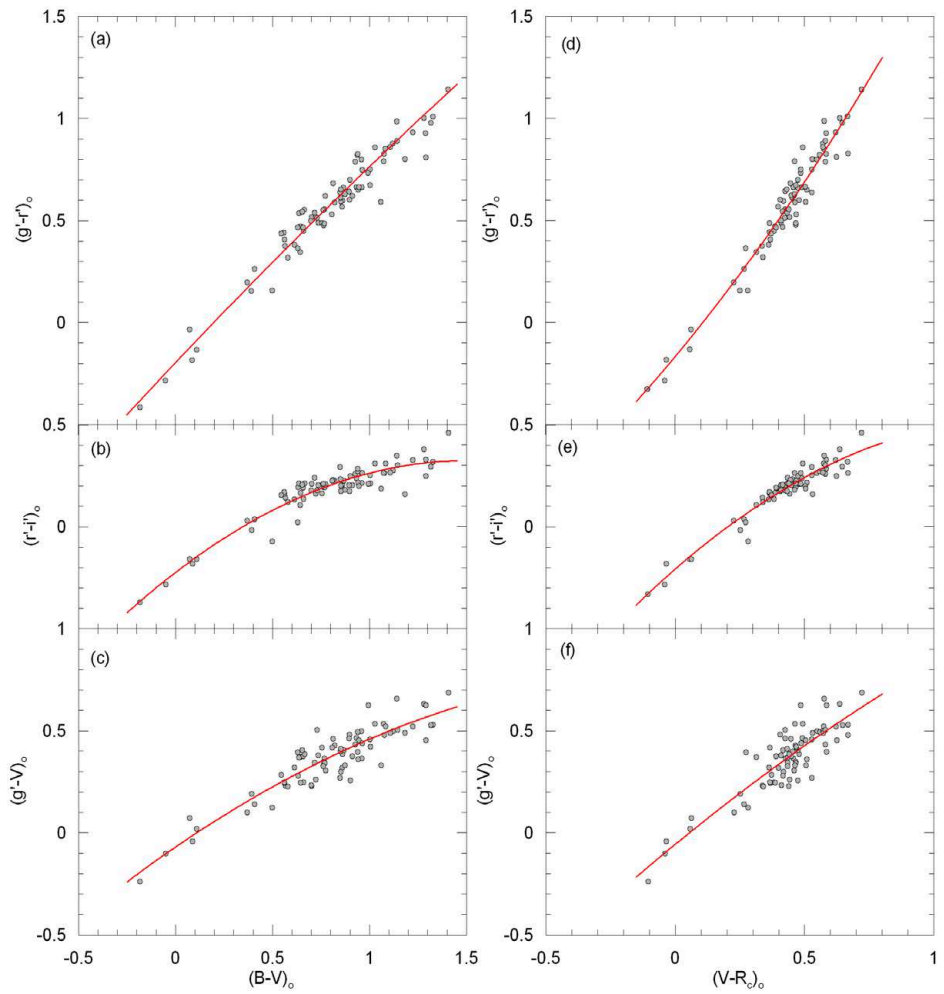


Figure 6: Distributions of the sample stars in six colour planes. The curves indicate quadratic polynomials.

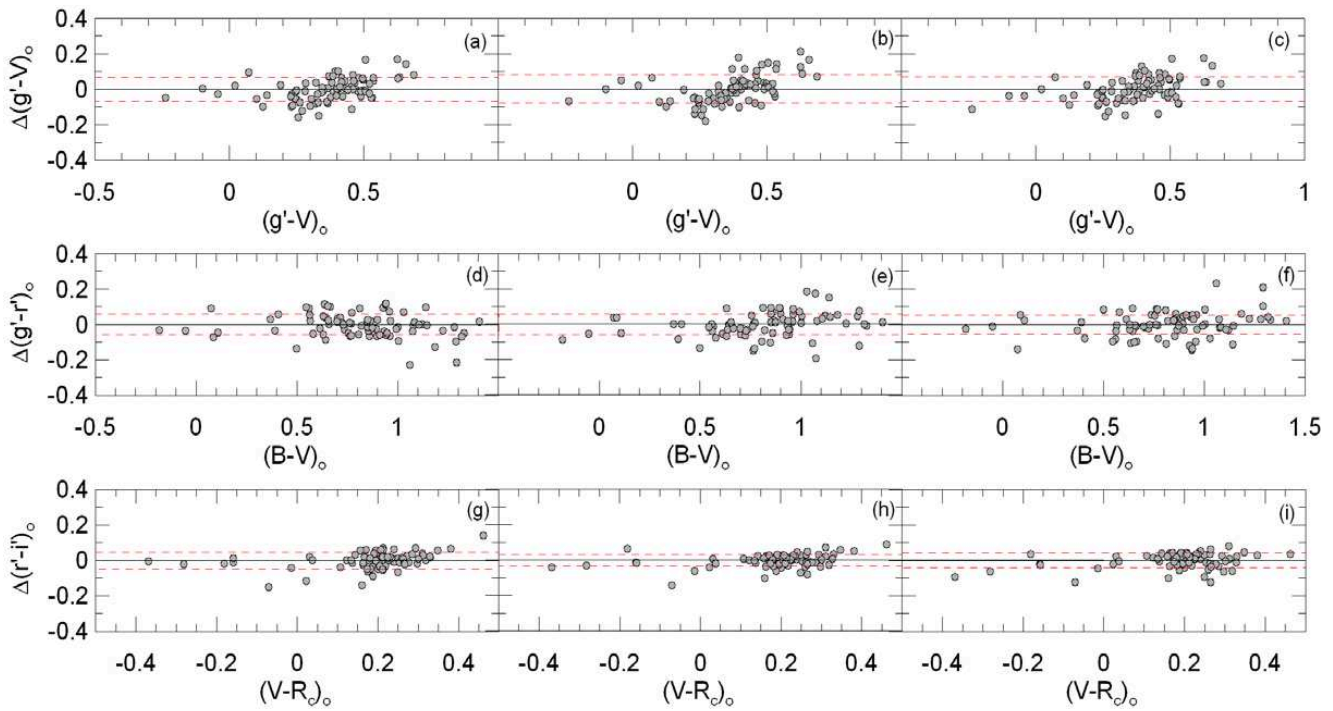


Figure 7: Distributions of the residuals of the sample stars for transformation equations (Eqs. 9-17).

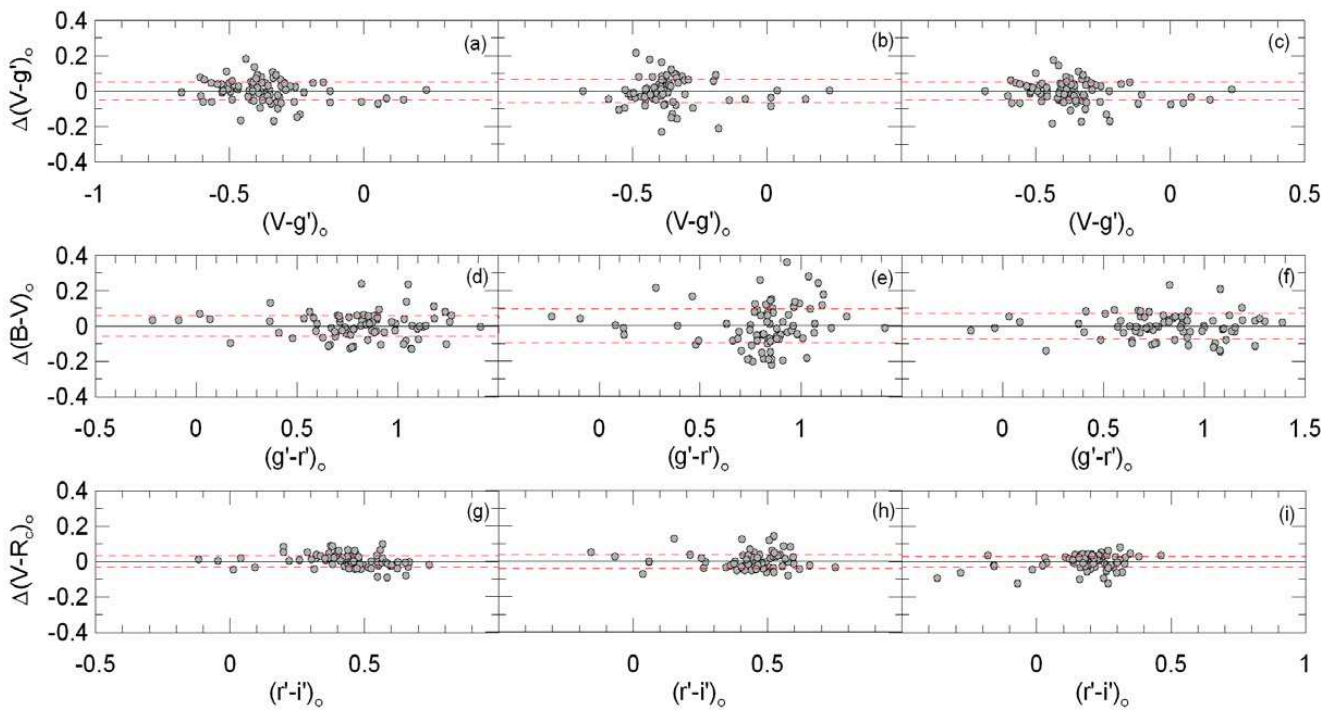


Figure 8: Distributions of the residuals of the sample stars for inverse transformation equations (Eqs. 18-26).

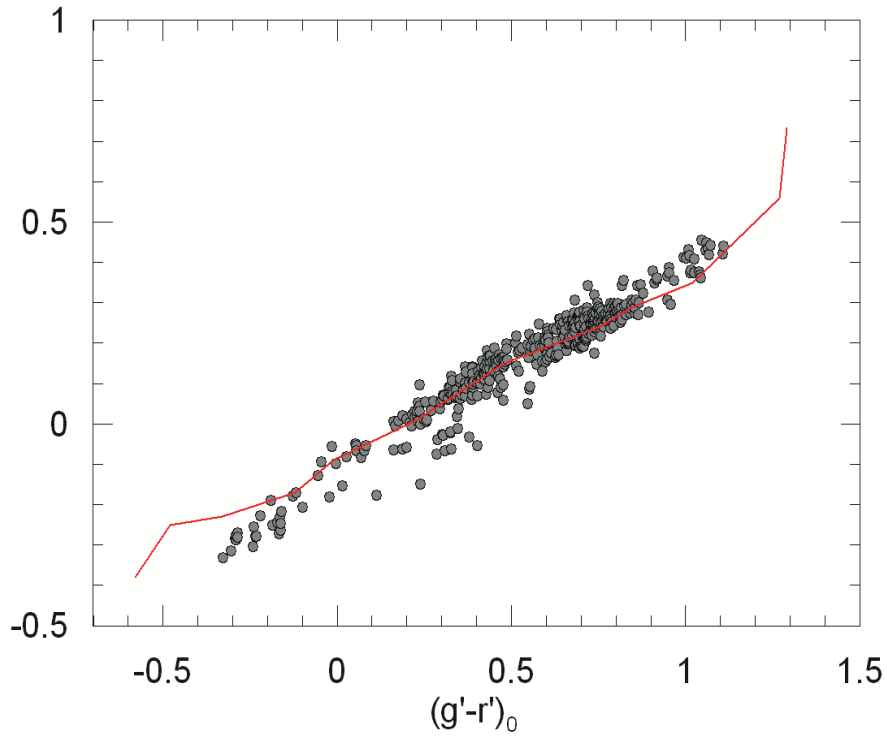


Figure 9: $(g' - r')_0 \times (r' - i')_0$ two-colour diagram of 427 stars used for the application of the transformation equations. The solid line indicates the synthetic two-colour diagram of Covey et al. (2007).

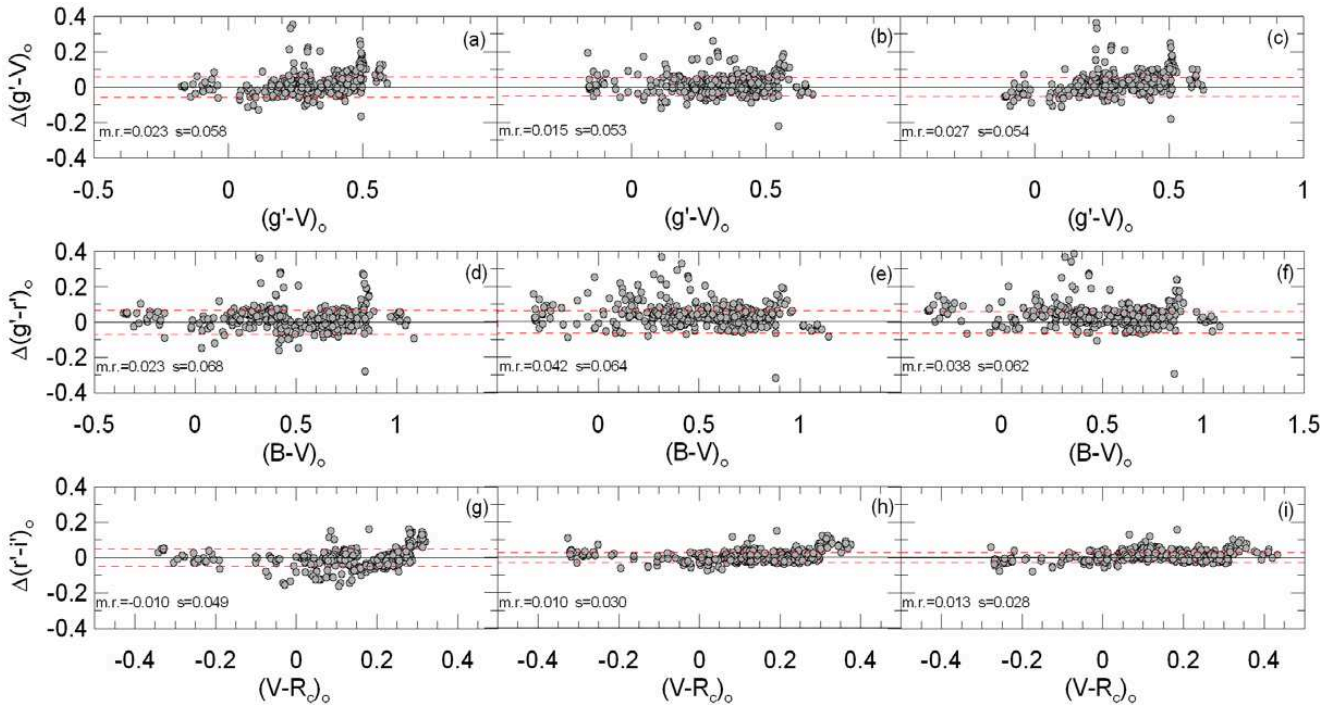


Figure 10: Distributions of the residuals of 427 stars used for the application of the transformation equations. Mean residuals ($m.r.$) and standard deviations (s) are also indicated in each panel.